

## Collective Excitations in the Dilute 2D Electron System

M. A. Eriksson,<sup>1</sup> A. Pinczuk,<sup>1,2</sup> B. S. Dennis,<sup>1</sup> S. H. Simon,<sup>1</sup> L. N. Pfeiffer,<sup>1</sup> and K. W. West<sup>1</sup>

<sup>1</sup>Lucent Technologies, Bell Labs, Murray Hill, New Jersey 07974

<sup>2</sup>Departments of Physics and Applied Physics, Columbia University, New York, New York 10027

(Received 22 October 1998)

We report inelastic light scattering measurements of dispersive spin and charge density excitations in dilute 2D electron systems reaching densities less than  $10^{10} \text{ cm}^{-2}$ . In the quantum Hall state at  $\nu = 2$ , roton critical points in the spin inter-Landau level mode show a pronounced softening as  $r_s$  is increased. Instead of a soft mode instability predicted by Hartree-Fock calculations for  $r_s \sim 3.3$ , we find evidence of multiple rotors in the dispersion of the softening spin excitations. [S0031-9007(99)08583-X]

PACS numbers: 73.20.Mf, 73.40.Hm, 78.30.Fs

As the density of a two-dimensional electron system decreases, unusual behavior is expected due to the increasing importance of the electron-electron interaction. Wigner originally predicted that at sufficiently low density an interaction driven phase transition to a crystal state would occur [1]. It is possible, however, that quantum phase transitions to other broken symmetry states may occur before the onset of crystallization. In the quantum Hall regimes, low energy rotors in collective excitations have been identified as possible precursors of instabilities at low electron densities [2–4]. Such collective excitations of quantum Hall systems have been observed using inelastic light scattering [5–7]. Until now, however, measurements have been restricted to high density systems, relatively far from predicted instabilities. In this Letter we report inelastic light scattering measurements of high mobility dilute 2D electron systems with densities less than  $10^{10} \text{ cm}^{-2}$ , in the range where instabilities have been predicted to occur [3].

In the quantum Hall regime breakdown of wave vector conservation due to weak residual disorder activates light scattering by critical points in the dispersion of collective modes, allowing the observation of roton minima in dispersion curves (Fig. 1c). We find that the roton of spin-density inter-Landau level (ILL) excitations at  $\nu = 2$  displays a significant softening at low density. At densities similar to those where Hartree-Fock calculations predict a zero-energy spin density mode [3], additional peaks appear in the light scattering spectra. These sharp peaks can be understood as the appearance of multiple rotors in the dispersion of the spin density excitation (SDE). We propose that the emergence of multiple rotors at very low density arises from a mixing of higher Landau levels into the ground state wave function. The roton instability of Hartree-Fock calculations seems to be removed or pushed to lower density by Landau level mixing in the ground state.

In light scattering with wave vector conservation we measure dispersive 2D plasmons (at magnetic field  $B = 0$ ) and charge density ILL excitations at  $B \neq 0$  (magnetoplasmons). Well-defined dispersions are observed at

densities  $n \leq 10^{10} \text{ cm}^{-2}$ . Because of the low electron density, we can measure the dispersions up to wave vectors approaching  $1/l_0$ , where  $l_0 = \sqrt{\hbar c/eB_\perp}$  is the magnetic length and  $B_\perp$  is the magnetic field normal to the sample.

The samples in this work are GaAs/ $\text{Al}_x\text{Ga}_{1-x}\text{As}$  single quantum wells containing high quality two-dimensional electron systems. In order to achieve low densities without gating the samples, we use heterostructure designs with large setbacks of the quantum well from the Si delta doping and very low aluminum concentrations in the barriers. The setbacks vary from 600 to 2400 Å, and the aluminum concentration varies from 10% down

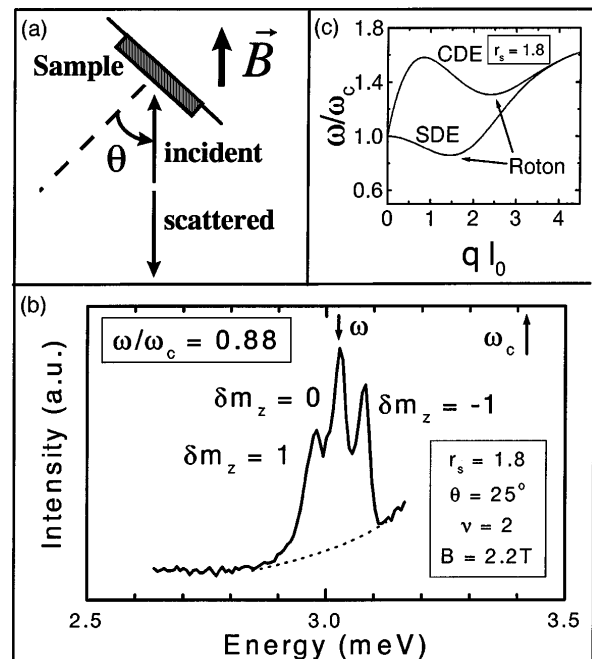


FIG. 1. (a) Experimental geometry. Changing the angle  $\theta$  changes the scattering wave vector  $q = \frac{4\pi}{\lambda} \sin \theta$ . (b) Depolarized inelastic light scattering spectrum of a sample with  $r_s = 1.8$  at  $\nu = 2$ . (c) Charge density and spin density excitations as a function of wave vector  $q$  in a Hartree-Fock approximation.

to 3%. The transport mobility of our samples exceeds  $1.5 \times 10^6 \text{ cm}^2/\text{Vs}$  at a density of  $1.3 \times 10^{10} \text{ cm}^{-2}$ . For more dilute samples, the dispersive plasmon is used to determine the electron density [8].

As shown in Fig. 1(a), light scattering spectra are acquired using a backscattering geometry at sample temperatures less than 200 mK. The angle  $\theta$  between the normal to the sample and the incident/scattered light is continuously tunable between  $\theta = \pm 60^\circ$  at low temperature, allowing the scattering wave vector  $q = \frac{4\pi}{\lambda} \sin \theta$  to vary between  $q_{\min} \approx 0$  and  $q_{\max} = 1.3 \times 10^5 \text{ cm}^{-1}$ . The laser excitation is kept close to the fundamental luminescence ( $\lambda_L = 8160 \pm 20 \text{ \AA}$ ) to provide resonant enhancement. Incident power densities are always lower than  $3 \times 10^{-4} \text{ W/cm}^2$ . More details on resonant light scattering may be found in Refs. [9]. It is convenient to define the electron density in terms of the usual dimensionless parameter  $r_s \equiv \frac{1}{\sqrt{\pi n}} \frac{m_b e^2}{\epsilon \hbar^2}$ , where  $m_b = 0.067$  is the band effective mass, and  $\epsilon = 13$  is the dielectric constant [10].

Inelastic light scattering mechanisms can be classified into two types: those that conserve wave vector  $q$ , and those that do not to conserve  $q$  [9]. Marmorkos and Das Sarma have written the intensity of scattering as  $I(q, \omega) \sim \int_0^\infty f_q(k) S_a(k, \omega) dk$ , where  $S_a(k, \omega)$  is the dynamical structure factor [11]. For the charge density response  $a = \rho$  and  $S_\rho$  is a density-density correlator; for the spin density response  $a = \sigma$  and  $S_\sigma$  is a spin-spin correlator.  $f_q(k)$  depends on the length scale and on the strength of the disorder. In the absence of disorder, or for long wavelength disorder, wave vector conservation is maintained:  $f_q(k)$  is sharply peaked at  $k = q$ , and  $I(q, \omega)$  maps out the dispersions of collective excitations. In the presence of short wavelength disorder,  $f_q(k)$  is broad, and light scattering is independent of  $q$ :  $I(\omega)$  is peaked at the energies of critical points in the density of states (DOS) for collective excitations. In intermediate cases, both critical points in the DOS and the wave vector conserving dispersion may be visible. In our samples and at integer quantum Hall states, we find that the light scattering for charge density excitations (CDEs) conserves wave vector when the setback  $d > 1600 \text{ \AA}$ , and breaks wave vector conservation when  $d < 1600 \text{ \AA}$ . When  $d \approx 1600 \text{ \AA}$  we observe both types of scattering.

Figure 1(b) shows a light scattering spectrum of ILL excitations in a sample with density  $n = 9.6 \times 10^{10} \text{ cm}^{-2}$ , corresponding to  $r_s = 1.8$ . The incident and scattered light have perpendicular polarizations (depolarized spectra), indicating that the light scattering peak is due to spin-density excitations [12]. Because of the spin symmetry at  $\nu = 2$ , the spin density inter-Landau level excitation is expected to be a triplet mode [2,3]. The sharp triplet of Fig. 1(b), whose components have a full width at half maximum less than  $20 \mu\text{eV}$ , is a direct observation of this degeneracy. The peaks in the triplet are labeled by the change in angular momentum  $\delta m_z$  parallel to the

magnetic field  $B$ , and their splitting is the Zeeman energy. We observe triplet excitations in all measured samples up to  $r_s = 3.3$ . At larger  $r_s$ , the Zeeman splitting is too small at  $\nu = 2$  to resolve the triplet.

The triplet in the depolarized spectra of Fig. 1(b) is shifted below the cyclotron energy  $\hbar\omega_c$  by 12%. As is the case for all depolarized spectra we report here, the light scattering in Fig. 1(b) is independent of angle  $\theta$  and wave vector  $q$ . Wave vector independence is the experimental signature of disorder activated scattering [13], so we identify the triplet as the roton minimum of the SDE, as shown in Fig. 1(c).

Figure 2(a) shows light scattering spectra of spin excitations at  $\nu = 2$  in a sample with  $r_s = 4.9$ . The two sharp peaks do not depend on angle  $\theta$ , indicating that they correspond to densities of states in the dispersion curves. Both peaks are shifted well below  $\hbar\omega_c$ . The two peaks do not correspond to  $\delta m_z$  components of the spin excitations, because the Zeeman energy is less than  $10 \mu\text{eV}$  at this field. The appearance of two such distinct peaks in light scattering spectra of the spin excitations at large  $r_s$  is surprising, because only a single critical point is expected in the dispersion of spin excitations [2,3,5].

The solid circles in Fig. 3 are the measured energies of spin density excitations at  $\nu = 2$  in 8 samples covering a

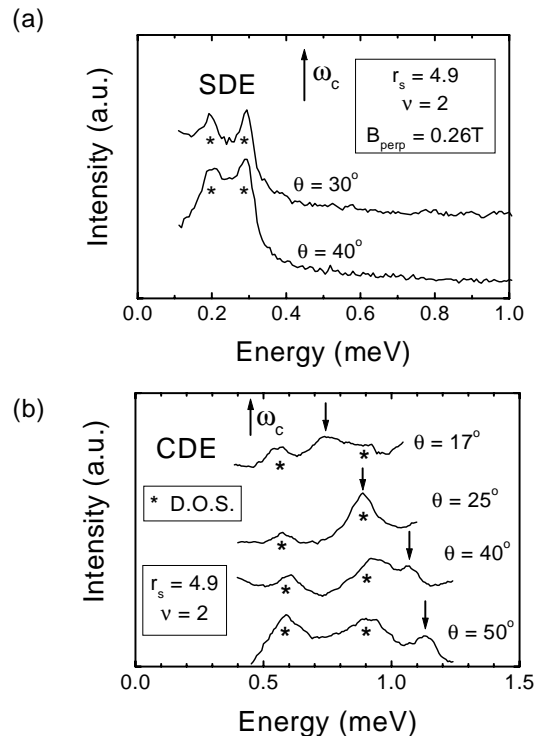


FIG. 2. (a) Two SDE peaks in a depolarized spectrum of a sample with  $r_s = 4.9$ . The peaks are split by much more than the Zeeman energy. (b) Polarized spectra from the same sample at four angles  $\theta$ . Stars indicate critical points activated by residual disorder, and downward arrows indicate the dispersive magnetoplasmon.

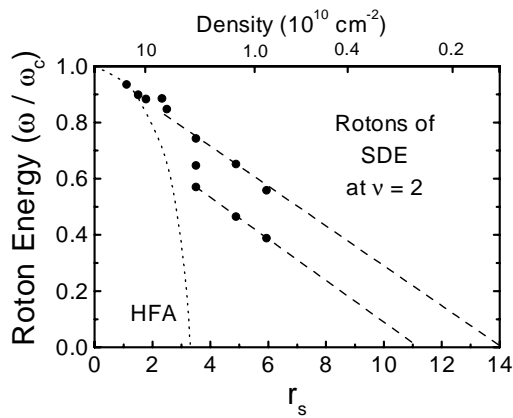


FIG. 3. Solid circles: Summary of peaks in depolarized spectra for eight samples, each with a different value of  $r_s$ . Peaks at the same value of  $r_s$  appear in the same sample. Note the onset of multiple peaks at  $r_s = 3.3$ . Dotted line: Calculated energy of the roton minimum in a Hartree-Fock approximation. Dashed lines: Linear extrapolation of the data.

wide range in  $r_s$ . We can compare these energies with a calculation in the Hartree-Fock approximation (HFA) of the energy of the spin-density roton minimum, shown as the dotted line in Fig. 3. The calculation includes both the effects of the finite thickness of the quantum well [14] and the self-consistent coupling between the excited states [3]. Although the fit is excellent for  $r_s < 2$ , the HFA predicts a collapse of the roton energy at  $r_s \approx 3.3$  which is not observed in our data. The HFA is perturbatively exact when  $r_s \ll 1$ , but is of questionable validity for  $r_s \gtrsim 1$ .

It is remarkable that the onset of multiple peaks in spin excitations, like the two peaks in Fig. 2(a), occurs at approximately the same value of  $r_s$  as the predicted HFA spin instability. Figure 3 shows that all the samples with  $r_s \geq 3.3$  have multiple peaks in depolarized spectra. The multiple peaks can be explained by the emergence of multiple rotors in the SDE dispersion at large  $r_s$ , which increase the number of critical points in the collective mode DOS. Multiple critical points produce multiple light scattering peaks. A naive extrapolation of the measured roton energies to larger  $r_s$ , as shown by the dashed lines in Fig. 3, reveals potential instabilities in the range  $11 \lesssim r_s \lesssim 14$ : although the HFA seems to overestimate the tendency towards instability, a spin instability may still occur before the anticipated transition to a Wigner crystal at even larger  $r_s$ .

Figure 4 shows how the concept of multiple rotors explains the depolarized (SDE) light scattering peaks we observe at large  $r_s$ . As shown in Fig. 1(c), however, the HFA predicts only a single roton minimum in the dispersion of spin excitations. The disagreement with Hartree-Fock calculations of the collective modes may arise because the HFA assumes *a priori* that the ground state at  $\nu = 2$  fills the lowest spin-split Landau level, without Landau level mixing. The origin of the single

roton minimum in the HFA is essentially the simple structure of the 0th and 1st (orbital) Landau level single particle wave functions, which have zero and one node, respectively. We suggest that the incorporation of higher Landau levels into the ground state at large  $r_s$  increases the complexity of the ground state wave function by including single particle states with a finite number of nodes. The finite number of nodes can lead to multiple rotors in the collective excitations. This is analogous to collective excitations at higher filling factors, which are predicted to have multiple rotors [2,3].

Figure 2(b) shows *polarized* spectra at four angles in the sample with  $r_s = 4.9$ . The light scattering peaks are due to the  $\nu = 2$  charge density excitation. Two peaks, marked by the  $\star$  under the peaks, are independent of  $\theta$  and are due to critical points in the density of states (DOS) for the CDE. Unlike all the spectra we have discussed so far, there is one peak in Fig. 2(b) which *does* depend on angle  $\theta$  and wave vector  $q$ . It is marked by the vertical arrows in Fig. 2(b). At  $25^\circ$  this peak overlaps the DOS peak at 0.9 meV. Previous experiments using inelastic light scattering to measure the CDE in the quantum Hall regime have utilized wave vector breakdown to measure densities of states [5], or have used gratings to determine a scattering wave vector [10,15]. In this sample, with  $r_s = 4.9$  and  $d = 1600 \text{ \AA}$ , we observe both wave vector conserving *and* wave vector nonconserving scattering in the same spectrum without artificial gratings. This crossover from nonconserving to conserving scattering is consistent with our earlier discussion of wave vector conservation breakdown. The data are also consistent with a shift in the spectral weight towards the magnetoplasmon mode which is expected at low density [16].

Figure 4 is a summary of depolarized and polarized light scattering in the sample with  $r_s = 4.9$ . The four asterisks indicate the energy of wave vector independent light scattering peaks, which arise from densities of states in the collective modes. The position of the asterisks

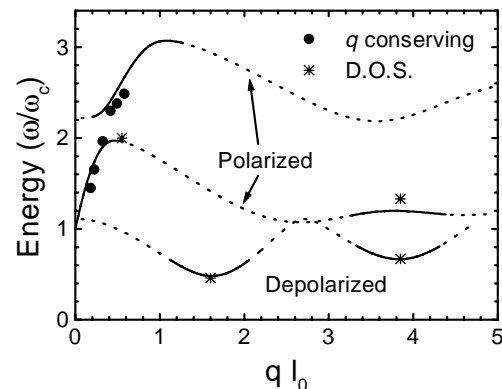


FIG. 4. Circles: Experimentally measured dispersion. Asterisks: Energies of observed critical points. Lines: SDE and CDE dispersions in a Fermi liquid theory approximation.

along the horizontal axis serves only to elucidate the discussion below. The solid circles represent the wave vector conserving peak, with  $q = \frac{4\pi}{\lambda} \sin \theta$ . The results in Fig. 4 provide a unique opportunity to compare both the critical points of the dispersion curves, and the low  $q$  dispersion itself, with theoretical calculations. Although the HFA was used with great success to calculate the mode dispersions at small  $r_s$ , it fails in the regime of large  $r_s$ . Specifically, the HFA predicts an unobserved zero-energy roton at  $r_s \approx 3.3$ ; it also predicts only a single roton minimum in SDE at all values of  $r_s$ , whereas our experiment shows multiple critical points. A robust approximation for large  $r_s$  electron systems is the Landau Fermi-liquid theory (FLT) [16,17]. We are led to apply FLT to our experiment because it provides a good method to treat the low density electron system at zero or small magnetic field  $B$ . In the same way that it was instructive to push the HFA out of its range of validity to large  $r_s$ , we find it useful to push the Fermi liquid theory out of its strict range of validity to large  $B$ , into the quantum Hall regime.

The lines in Fig. 4 represent the calculated dispersions of spin and charge modes in a semiclassical FLT approximation using only the first significant Fermi liquid parameters for charge,  $F_1^s$ , and spin,  $F_0^a$  [18]. We recall that  $F_1^s$  and  $F_0^a$  determine the effective mass and the spin susceptibility, respectively. The best fit to our data is obtained with  $F_1^s = -0.1$  and  $F_0^a = -0.87$ , which are not unreasonable values for these parameters at this density [19]. We mark with thick lines the regions where the weight of the collective mode is large in the dynamical structure factor  $S_a(q, \omega)$ . The weight in  $S_a(q, \omega)$  oscillates because of variations in the commensurability of the cyclotron orbits and the wave vector of the collective oscillation; this is analogous to the variation in the matrix elements for the overlap of particle-hole pairs in HFA calculations. The dispersive peak represented by the solid circles in Fig. 4 is revealed to be the dispersive magnetoplasmon. The weight in  $S_a(q, \omega)$  continues through the avoided crossing at  $\sim 2.1$  meV, as observed in the experiment [20]. The two critical points in the spin (charge) mode are explained as arising from two minima (maxima) in the dispersions. The variation in the weight of  $S_a(q, \omega)$  explains why peaks are observed at only specific flat regions of the dispersion curves.

The surprisingly good numerical agreement (only two fitting parameters were used,  $F_1^s$  and  $F_0^a$ ) between our data and the FLT calculations must at this point be regarded as fortuitous. Neither FLT nor the HFA are fully valid in our experimental regime. While the HFA provides an excellent treatment of the  $\nu = 2$  quantum Hall system with weak interactions, it is expected to fail in the strong interaction limit. Conversely, although FLT is an excellent paradigm in which to treat strong interactions in weak magnetic fields, it is not well suited to handling the fully quantum limit at  $\nu = 2$ .

We studied dilute 2D electron systems by means of inelastic light scattering. The magnetoplasmon shows a well-defined dispersion in the quantum Hall regime down to  $n < 10^{10} \text{ cm}^{-2}$ . At  $\nu = 2$  the roton of the spin-density mode softens at large  $r_s$ . The spin instability predicted by HFA calculations at  $r_s \sim 3.3$  is not observed, but we find the emergence of multiple rotons in the spin-density mode. We suggest a mixing of higher Landau levels in the ground state wave function as an explanation for the appearance of multiple rotons at large  $r_s$ . The collapsing energy of the roton of spin excitations suggests the possibility of instabilities at large  $r_s$  due to spin correlations, in addition to the anticipated Wigner crystal.

We thank K. Todd and J. P. Eisenstein for calculating the charge density in the growth direction of our samples.

- 
- [1] E. P. Wigner, *Phys. Rev.* **46**, 1002 (1934).
  - [2] C. Kallin and B. I. Halperin, *Phys. Rev. B* **30**, 5655 (1984).
  - [3] A. H. MacDonald, *J. Phys. C* **18**, 1003 (1985).
  - [4] S. M. Girvin, A. H. MacDonald, and P. M. Platzman, *Phys. Rev. B* **33**, 2481 (1986).
  - [5] A. Pinczuk *et al.*, *Phys. Rev. Lett.* **61**, 2701 (1988); A. Pinczuk *et al.*, *Phys. Rev. Lett.* **68**, 3623 (1992).
  - [6] A. Pinczuk *et al.*, *Phys. Rev. Lett.* **70**, 3983 (1993); A. Pinczuk *et al.*, *Physica (Amsterdam)* **249B**, 40 (1998).
  - [7] H. D. M. Davies *et al.*, *Phys. Rev. Lett.* **78**, 4095 (1997).
  - [8] M. A. Eriksson *et al.*, in *Proceedings of the ICPS, 1998*, Vol. 24.
  - [9] *Light Scattering in Solids IV*, edited by M. Cardona and G. Guntherodt, *Topics in Applied Physics* Vol. 54 (Springer-Verlag, New York, 1984); A. Pinczuk *et al.*, *Philos. Mag. B* **70**, 429 (1994).
  - [10] T. Ando, A. B. Fowler, and F. Stern, *Rev. Mod. Phys.* **54**, 437 (1982), and references therein.
  - [11] I. K. Marmorosk and S. Das Sarma, *Phys. Rev. B* **45**, 13396 (1992).
  - [12] Y. Yafet, *Phys. Rev.* **152**, 858 (1966); E. Burstein *et al.*, *Surf. Sci.* **98**, 451 (1980).
  - [13] A flat dispersion near  $q = 0$  shifted down 12% from  $\omega_c$  could also lead to a  $q$ -independent signal. However, the HFA is excellent at high density and predicts no such shift, making this interpretation unlikely. The low density data discussed later are in a qualitatively new regime, so it is conceivable, but unlikely, that one of those peaks may arise from the  $q \approx 0$  dispersion.
  - [14] C. Kallin, in *Interfaces, Quantum Wells, and Superlattices*, edited by C. R. Leavens and R. Taylor (Plenum, New York, 1988), p. 163.
  - [15] L. L. Sohn *et al.*, *Solid State Commun.* **93**, 897 (1995).
  - [16] D. Pines and P. Nozieres, *The Theory of Quantum Liquids* (Addison-Wesley, New York, 1966).
  - [17] T. K. Lee and J. J. Quinn, *Phys. Rev. B* **11**, 2144 (1975).
  - [18]  $F_0^s$  has little effect at large  $r_s$ , so we set  $F_0^s = 0$ .
  - [19] Y. Kwon *et al.*, *Phys. Rev. B* **50**, 1684 (1994), and references therein.
  - [20] E. Ulrichs *et al.*, *Phys. Rev. B* **56**, R12760 (1997).